GIANT HERBIG-HARO FLOWS

JOHN BALLY AND DAVID DEVINE
Center for Astrophysics and Space Astronomy,
University of Colorado, Boulder CO 80309, USA

Abstract. Recent observations with wide field-of-view CCDs have shown that over 20 Herbig-Haro flows extend for more than one parsec from their driving sources. We review the observed properties of these giant HH flows and discuss the physical consequences for star formation, and for the physics and chemistry of the surrounding interstellar medium.

1. Introduction

The advent of large format (2048 × 2048 pixels or larger) CCD detectors have for the first time provided both high sensitivity (orders of magnitude greater than photographic emulsions) *and* a wide field-of-view (FOV) approaching one degree. The combination of these two parameters has opened opportunities for deep narrow-band imaging of entire star forming clouds. Such observations have shown that many Herbig-Haro (HH) objects trace parse-scale outflows from young stars.

The first parsec-scale Herbig-Haro flow was recognized in 1993 (Bally & Devine 1994) with the 23′ FOV provided by a Tektronix 2k CCD on the KPNO 0.9-m telescope. The HH34 jet (Reipurth et al. 1986) in the Orion A molecular cloud was found to power a 20′ long chain of HH objects with a projected length of 3 parsecs (assuming a distance of 500 pc). This system, containing the previously discovered objects HH33/40, HH34, H34N, HH85/86/87, HH126, and a new object HH173, is powered by a less than $45L_{\odot}$ young stellar object (YSO), HH34 IRS. High quality images of the entire system, obtained with the ESO NTT in January 1994, were compared with images taken in the 1980s with a variety of telescopes to determine proper motions of various knots. These measurements together with R = 6000 resolution long-slit spectra demonstrate that all HH objects north of HH34 IRS move north and are redshifted while all HH objects to the south

B. Reipurth and C. Bertout (eds.), Herbig–Haro Flows and the Birth of Low Mass Stars, 29–38.

of HH34 IRS move south and are blueshifted (see images in Devine 1997; Devine et al. 1997). Radial velocities and proper motions show systematic decrease in velocity with increasing distance from the source. The flow morphology and kinematics exhibits S-shaped point symmetry indicating possible long-term changes in the ejection direction of the bipolar jet from HH34 IRS. High velocity CO emission is confined to the inner 0.1 pc portion of the parsec-scale optical flow. However, shock excited H_2 emission has been detected near the flow ends 1.5 pc from the source (HH85 and HH33/40 in the north; HH86/87/88 in the south), but not in the internal working surfaces closer to the HH34 IRS (see Devine et al. 1997 for details).

Wide FOV imaging of other star forming clouds have demonstrated that parsec-scale HH flows are common with lengths ranging from 1 to over 10 parsecs. Some of the best known and most studied molecular outflows and HH objects contain shocks lying more than 1 pc from their sources. Ogura (1995) reported a parsec-scale flow associated with HH1/2 that contains a 0.5 pc diameter shock close to the HH1/2 outflow axis, HH401, and a counter-shock HH 402 to the southeast of HH1/2 directly opposite HH401. This flow has a projected end-to-end length of about 6 parsecs. Barnard 5 IRS1, the source of a well known molecular outflow, powers a spectacular pair of HH objects (HH366) lying beyond the projected edges of the B5 cloud about $10'$ on either side of the source (Bally, Devine, & Alten 1996). Re-analysis of existing millimeter wavelength data shows that the CO flow is co-extensive with the optical flow and much larger than previously thought. The HH111 flow contains HH311 and HH113 (Figure 1), which lie more than 3.8 pc on either side of the VLA source (Reipurth, Bally, Devine 1997). In this case, the optical flow is almost 10 times larger than the associated molecular flow, which is confined to the inner 1 parsec portion of this system (cf. Cernicharo & Reipurth 1996 and references therein). The T-Tauri system is the source of a giant bow shock HH355N which subtends more than 0.2 square parsecs and lies nearly one parsec from the source, and a similar counter bow shock HH 355S on the opposite side of T Tauri; both are seen in Figure 2 (Reipurth, Bally, Devine 1997). The counter-jet in the HH83 system appears to power several shocks lying between it and HH 84, the apparent terminal shock of this flow located more than 3 parsecs from the source at the western edge of the Orion A molecular cloud. Some bow shocks powered by YSOs in L1551 lie well beyond the projected extent of detectable CO emission in regions with such low extinction that galaxies can be seen in the background. Most (but not all) parsec-scale flows discovered to date are powered by low mass YSOs.

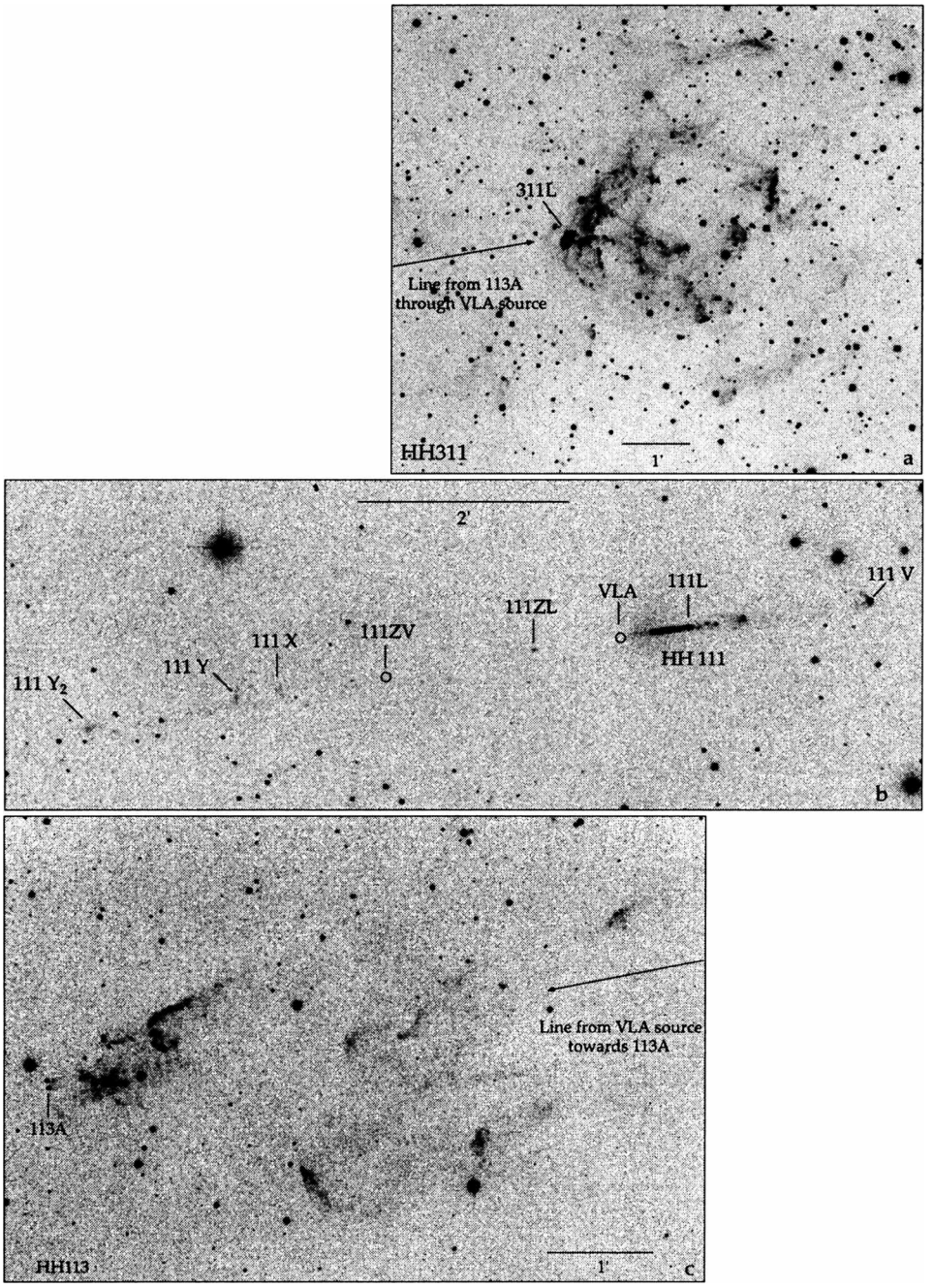

Figure 1. Close-up views of the three major components of the 7 pc long HH111 flow. *Upper Right:* NTT Hα + [S II] image showing HH311 located 3.8 pc west of HH111. *Center:* KPNO 0.9 m [S II] image of the HH111 jet and counter jet. *Bottom Left:* NTT Hα + [S II] image showing HH113 located 3.5 pc east of HH111. Proper motions show that these HH objects are moving away from the source of HH111. The eastern object, HH113, is redshifted and the western object, HH311, is blueshifted. From Reipurth, Bally, Devine (1997).

https://doi.org/10.1017/S0074180900061519 Published online by Cambridge University Press

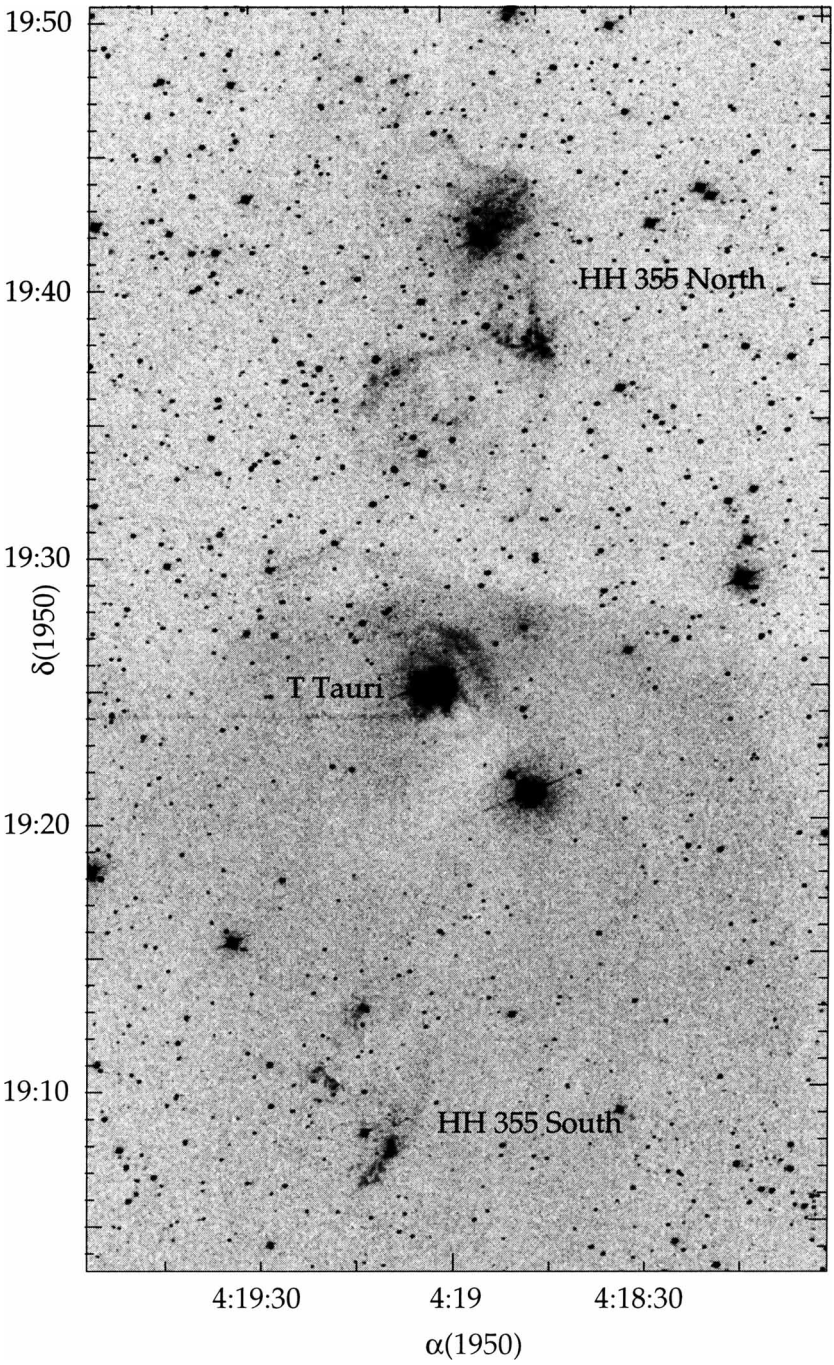

Figure 2. The T-Tauri parsec-scale Herbig-Haro flow, HH355, showing a giant bow shock extending 20′ to the north and a chain of HH objects extending 20′ to the south. From Reipurth, Bally, Devine (1997).

https://doi.org/10.1017/S0074180900061519 Published online by Cambridge University Press

2. Observed Properties

Table 1 lists some giant HH flows and their sizes. In this section, we describe the observed properties of these flows.

Large Dynamic Ages: The dynamical ages of parsec-scale outflows are about an order of magnitude larger than the ages of the previously recognized Herbig-Haro flows. A typical dynamical age for a shock in a parsec scale Herbig-Haro flow is $\tau_{dyn} = 10^4\ d_{pc}/v_{100}$ years, where d_{pc} is the flow length in parsecs and v_{100} is the apparent velocity in units of 100 km s^{-1}. For the flows discussed here, the dynamical ages of the outermost visible components range from 10^4 to 10^5 years. The longer time scale is comparable to the estimated duration of both the stellar accretion phase and the lifetimes of outflows estimated from CO observations.

Multiple Internal Working Surfaces: Most giant HH flows contain multiple groups of HH objects along the outflow axis, providing evidence for time-variable ejection velocity, ejection direction, and possibly mass-loss rate and degree of collimation. The spacing of shocks tends to increase with increasing distance from the source. Some HH flows contain continuous jets within 0.1 pc of the source. Others have closely spaced shocks separated by several arc minutes in the inner parsec of the flow. Most have large gaps between the outermost shocks that can be up to 10′ long. The ratio of the observed proper motions divided by the shock velocity deduced from the emission lines is much larger than unity, indicating that most HH objects are shocks formed by faster fluid elements overtaking moving fluid with a slightly lower velocity and *not* stationary gas. Thus, most HH objects are internal shocks that trace interactions between plugs of material ejected at different times with different velocities from a YSO.

S-Shaped Point Symmetry: Many parsec-scale flows have S-shaped point symmetry about the source. Either precession or irregular source orientation changes can lead to S-shaped symmetry. Examples include HH34 and PV-Ceph (Figure 3). At least one source (B5; Bally, Devine, & Alten 1996) has C-shaped symmetry indicating either flow deflection or relative motion of the source and the medium into which the flow is propagating.

Velocities, Sizes, Morphologies: There is a systematic decrease in the mean fluid velocities as determined from both proper motion and radial velocity measurements (cf. HH34; Devine 1997). There is an increase in the linear dimensions of HH objects with increasing distance from the source. Furthermore, shocks look increasingly complex and chaotic with increasing distance from the source.

Blow-Out: Parsec-scale flows have sizes about an order of magnitude larger than the cloud cores from which they originate. Many flows have punched completely out of their parent molecular cloud cores and are in-

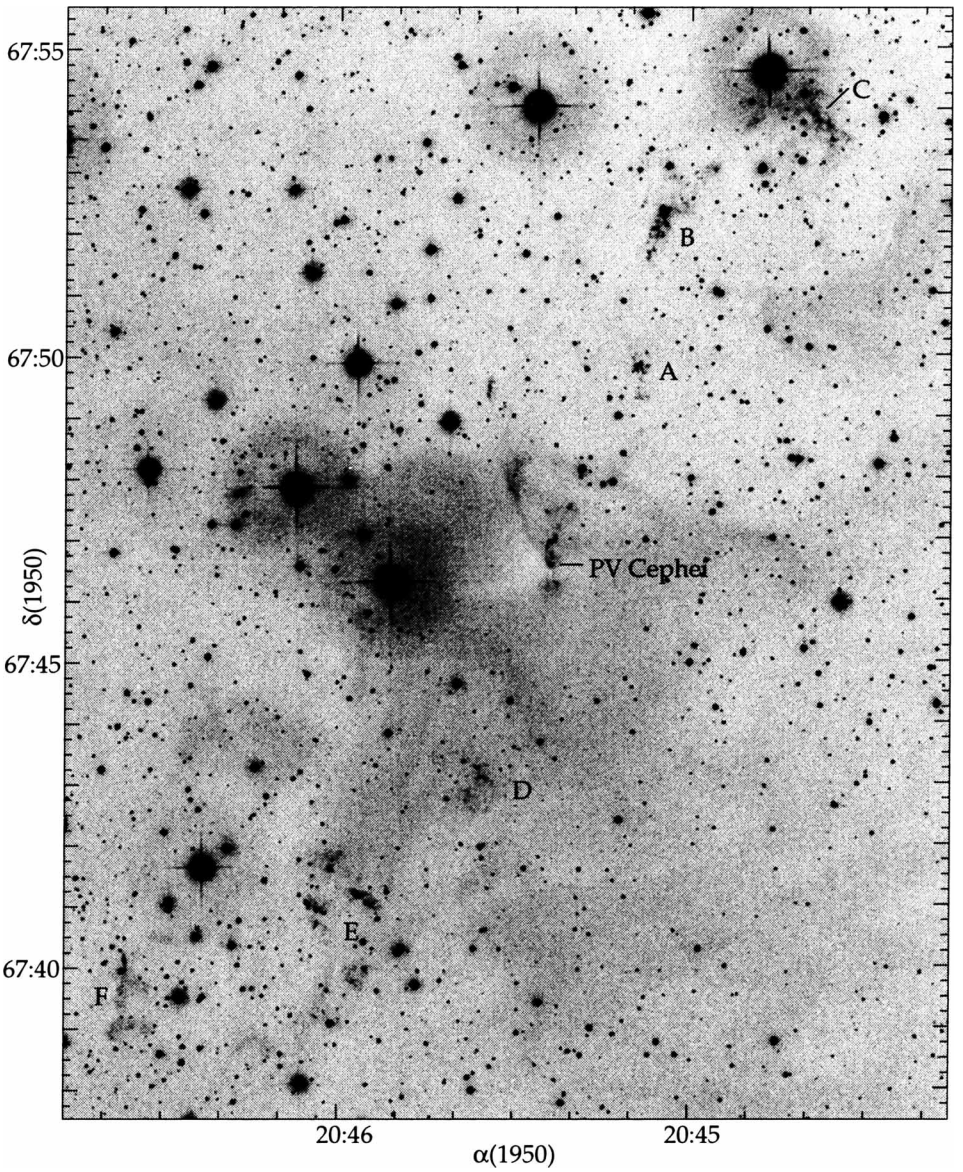

Figure 3. A KPNO 0.9 meter image of the 20′ PV-Ceph parsec-scale HH315 flow (chain of nebulae extending along a northwest – southeast axis) showing S-shaped symmetry about the source. A second flow may emerge from the cloud core towards the northeast. From Reipurth, Bally, Devine (1997).

https://doi.org/10.1017/S0074180900061519 Published online by Cambridge University Press

jecting mass and energy into the surrounding atomic or ionized interstellar medium. For example, the northern shock in the T Tauri system, the northeastern shocks in the L1551 IRS5 system, and HH311, the western terminus of the HH111 system, lie along a lines-of-sight devoid of CO emission that contain a rich distribution of background stars and galaxies.

Clustering: Most giant HH flows listed in Table 1 were found in regions of relatively isolated star formation such as L1551 which contain about a dozen or fewer YSOs. Even in these regions, there is evidence for multiple outflows that frequently overlap in the plane of the sky. However, many (possibly most) YSOs are found in highly clustered environments where many dozens to hundreds of stars have formed within a parsec-scale region. In such environments, it is hard or impossible to make specific associations between individual HH objects and sources. Images of the Perseus cloud complex reveal many HH objects located more than a parsec from the nearest known YSO or cloud core. Owing to confusion, many such HH objects have not yet been linked to specific flows or sources (cf. NGC1333; Bally, Devine, & Reipurth 1996: L1448 and L1455; Bally et al. 1997).

3. Consequences of Parsec-Scale Herbig-Haro Flows

Our observations demonstrate that HH objects are frequently found parsecs from their driving sources. Therefore, outflows traced by HH objects have physical dimensions at least an order of magnitude larger than previously thought. The large sizes of outflows from low mass stars has a number of implications.

Implications for Outflow Models: The fast component of outflows that excite HH objects can be traced at least as far from their driving sources as associated molecular outflows. In some cases, the optical outflow is an order of magnitude larger than the associated CO flow. Such observations provide support for "unified" outflow models in which a fast, collimated, time-dependent, and bipolar wind (or jet) from a YSO that excites HH objects is also the primary engine that powers the lower velocity lobes traced by CO (Raga & Cabrit 1993; Masson & Chernin 1993, 1994; Chernin et al. 1994). In this model, molecular gas is entrained by the jet from the environment. Collimated and time-variable jets can produce poorly collimated lower velocity molecular outflows by the combined action of jet orientation variations (precession) and velocity variations. As jets change their orientation, they constantly encounter fresh material which is entrained and accelerated. An outflow cavity with a relatively wide opening angle can be produced. Ejection velocity variations produce multiple internal shocks where fast fluid elements overtake slower moving ejecta (e.g. Biro & Raga 1994; Raga & Kofman 1992). The resulting 'splash' of post-

shock debris spreads orthogonal to the mean flow axis and can contribute to the widening of the flow cavity and the entrainment and acceleration of displaced gas.

Mass-Loss History of YSOs: The morphology and kinematics of parsec-scale flows can be used to constrain the mass loss history of the source YSOs and to probe the evolution of HH objects. Shocks in parsec-scale outflows trace ejecta that are progressively older with increasing distance from the source. The apparent deceleration of the distant ejecta may be a result of interactions with slower moving (or stationary) material in the outflow cavity. Alternatively, older, more distant material may have been ejected at a lower velocity than more recent ejecta. If the latter interpretation is correct, then the mean jet ejection velocity must have changed significantly in the lifetimes of the visible outflow components. With detailed radial velocity, proper motion, and excitation data, it may be possible to partially reconstruct the mass ejection history of the source YSO, and by inference, its mass accretion history. The distribution of shocks (continuous jets or many closely spaced low excitation shocks near the source and widely spaced higher excitation ones farther away) implies that flow velocity variations with low amplitudes occur frequently while large amplitude variations are relatively rare. The inverse correlation between ejection velocity jumps and their frequency is reminiscent of a $1/f$ process.

Probing the ICM and ISM with HH Objects: Most of the volume inside giant molecular clouds is filled with voids that do not emit strongly in the CO lines. The nature of this inter-clump medium (ICM) remains mysterious. The terminal working surfaces of giant HH flows can be used to probe the nature of the ICM. Analysis of the shock properties can provide information about the ionization state, density, and other physical characteristics of the ICM. For instance, detection of shock excited H_2 can be used to infer that the pre-shock medium is predominantly molecular; the presence of Balmer filaments would be an indication that the shock is moving into a neutral atomic medium.

Chemical Rejuvenation: Fast shocks associated with the terminal working surfaces of parsec-scale flows may dissociate molecules, resulting in the 'chemical rejuvenation' of star forming molecular clouds. Dissociation of molecules effectively re-sets the conditions of the effected region to its 'initial' atomic state. Furthermore, shocks may contribute to the production of the large abundance of species such as C I and C II found in the ICM even if UV radiation from O and B stars is absent. Chemical rejuvenation must be an important process in the vicinity of young clusters such as NGC1333 where dozens of active flows can simultaneously churn the surrounding medium and where the mean time between the passage of dissociating shocks over random parcels of gas can be short compared to

the dynamic evolutionary time scale of the cloud.

Origin of Turbulence and Self-Regulation of Star Formation: Parsec-scale outflows may be the primary agents for the generation of turbulence in molecular clouds and the surrounding ISM in the absence of massive stars. They may contribute to the self-regulation of star formation. Giant flows sweep-up and expel gas from the parent cloud core, inject it into the surrounding ICM, and, in cases where the source lies near the edge of a molecular cloud, into the surrounding interstellar medium. If the ambient medium is predominantly atomic, the swept up gas will not be traceable by molecular emission lines, and the HH flow may extend much farther than any associated molecular outflow. However, if the ambient medium is predominantly molecular, an extended molecular outflow is produced. The classical molecular outflows are likely to be accelerated during the initial stages of this process and much lower velocity large scale flows formed during the latter stages. Eventually these mass motions degrade in momentum conserving interactions with their surroundings and eventually blend with the surrounding medium. The non-linear growth of instabilities during the earlier radiative phases will likely make the final state chaotic and turbulent.

Prospects for X-Ray and UV-Observations: The 'naked' portions of giant flows, where galaxies can be seen in the background, may be observable at X-ray and UV wavelengths. Emission produced by fast shocks or absorption lines originating from high ionization states of various elements may be observable. Shock-excited emission may make a substantial contribution to X-ray and UV backgrounds of the Galaxy and provide a new probe of the star formation environment. Since velocities in the ambient medium are typically only a few kms^{-1}, the shock velocity in terminal working surfaces reflects the full flow velocity. Assuming that thermal and ionization equilibrium is reached and that the fluid velocity has declined by a factor of f in propagating through the outflow cavity, the immediate post-shock temperature in the adiabatic layer that forms behind either the bow or reverse shock (depending on the density contrast between the ambient and moving fluids) will attain a value $T_{ps} > 0.08\mu m_H f^2 v_0^2/k \approx 3 \times 10^5 V_{300}^2 f_{0.5}^2$ Kelvin. For the faster flows (such as HH 111), this implies terminal post-shock temperatures of at least 10^6K. Since the density in the inter-clump medium of a GMC, or in the ISM that surrounds it, can be as low as 0.1 cm^{-3}, the cooling time for the hot component may approach the dynamical time scales of the flow. Conditions in the terminal shocks of parsec scale flows that punch into relatively low density environments may resemble those found in moderately old supernova remnants and the same shock diagnostics may be applied.

TABLE 1. Some Parsec-Scale Herbig-Haro Flows

Flow	Coordinates (B1950.0)	Angular Size (l)	Projected Size (parsecs)
L1448 (IRS2)	$03^h\ 22^m$, $+30^o\ 35'$	~20	$\sim 1.8 \times d_{300}$
L1448 (IRS3)	$03^h\ 23^m$, $+30^o\ 35'$	~30	$\sim 2.7 \times d_{300}$
B5 IRS1 (HH366)	$03^h\ 44^m$, $+32^o\ 43'$	22	$1.9 \times d_{300}$
IRAS04239+2436 (HH300)	$04^h\ 24^m$, $+24^o\ 36'$	> 29	$> 1.1 \times d_{150}$
T-Tauri	$04^h\ 19^m$, $+19^o\ 25'$	40	$1.8 \times d_{150}$
L1551 IRS5	$04^h\ 29^m$, $+18^o\ 02'$	32	$1.4 \times d_{150}$
HH114/115	$05^h\ 15^m$, $+07^o\ 07'$	19	$2.6 \times d_{500}$
HH243 (RNO43)	$05^h\ 30^m$, $+12^o\ 48'$	26	$3.8 \times d_{500}$
HH83/84	$05^h\ 32^m$, $-06^o\ 31'$	>20	$> 2.9 \times d_{500}$
HH34	$05^h\ 33^m$, $-06^o\ 29'$	20	$2.9 \times d_{500}$
HH1/2 + HH401/402	$05^h\ 34^m$, $-06^o\ 48'$	43	$6.2 \times d_{500}$
HH111	$05^h\ 49^m$, $+02^o\ 48'$	57	$7.7 \times d_{500}$
Z CMa	$07^h\ 01^m$, $-11^o\ 28'$	10.7	$3.6 \times d_{1150}$
HH80/81	$18^h\ 16^m$, $-20^o\ 49'$	>12	$> 5.3 \times d_{1500}$
PV-Ceph	$20^h\ 45^m$, $+67^o\ 46'$	19	$2.6 \times d_{500}$
L1228 (HH199)	$20^h\ 58^m$, $+77^o\ 24'$	20	$1.8 \times d_{300}$
L1228 (HH200)	$20^h\ 58^m$, $+77^o\ 25'$	18	$1.6 \times d_{300}$

Acknowledgements: We thank Bo Reipurth for his collaboration on this project. This research was partially funded by NASA grants NASA grant NAGW-4590 (Origins) and NASA grant NAGW-3192 (LTSA).

References

Bally, J., & Devine, D. 1994, ApJ, 428, L65
Bally, J., Devine, D., Alten, V., & Sutherland, R. S. 1997, ApJ, 478, 603
Bally, J., Devine, D., & Alten, V. 1996, ApJ, 473, 921
Bally, J., Devine. D., & Reipurth, B. 1996, ApJ, 473, L49
Biro, S., & Raga, A. C. 1994, ApJ, 434, 221
Cernicharo, J., & Reipurth, B. 1996, ApJ, 460, 57
Chernin, L. M., Masson, C. R., Pino, E. M. G. D., & Benz, W. 1994, ApJ, 426, 204
Devine, D., Bally, J., Reipurth, B. & Heathcote, S. 1997 AJ (in press)
Devine, D. 1997, in *Low Mass Star Formation - from Infall to Outflow: Poster Proceedings of IAU Symposium No. 182*, ed. F. Malbet, A. Castets, p. 95
Masson, C. R., & Chernin, L. M. 1993, ApJ, 414, 230
Masson, C. R., & Chernin, L. M. 1994, 1994, Ap&SS, 216, 113
Ogura, K. 1995, ApJ, 450, 23
Raga, A. C., & Kofman, L. 1992 ApJ 386, 222
Raga, A. C., & Cabrit, S. 1993 A&A, 278, 267
Reipurth, B, Bally, J., Graham, J. A., Lane, A. P., & Zealey, W. J. 1986, A&A, 164, 51
Reipurth, B., Bally, J., Devine, D. 1997, AJ, in press